Paste 2026 – AB Fourie, M Horta, M Oliveira & S Wilson (eds)

doi:10.36487/ACG_repo/2655_17

# Consolidation evaluation of tailings slurry considering rock mass drainage properties in underground stopes

**Qinghai Ma [a,b], Guangsheng Liu [a,b,*], Xiaocong Yang [a,b], Lijie Guo [a,b]**

[a] *BGRIMM Technology Group, Beijing, China*

[b] *National Centre for International Research on Green Metal Mining, China*

## Abstract

*In open stoping with subsequent backfill mining, the backfilled tailings slurry in one stope is typically surrounded by the rock mass in adjacent stopes. The rock mass generally contains geological faults and joints that can serve as drainage pathways for water seepage within the backfill slurry during its consolidation process. However, the effects from the adjacent rock mass were traditionally simplified to be a totally impermeable or permeable boundary in previous studies. In this paper, numerical modellings with FLAC3D were firstly conducted to investigate the influences of hydro-geotechnical properties of surrounding rock mass on consolidation process of the uncemented tailings slurry in a vertical stope. Results show that the porewater pressure (PWP) and effective stresses of the slurry confined by rock mass are consistently higher than those obtained by assuming fully permeable boundaries, but obviously lower than those derived from impermeable boundary assumptions. A five-fold difference in peak PWP and effective stresses occurs when the rock mass hydraulic conductivity varies within common ranges from $10^{-8}$ m/s to $10^{-5}$ m/s. It is reasonable to simply understand the rock mass to be an impermeable boundary with a hydraulic conductivity lower than $10^{-8}$ m/s and a permeable boundary when it has a high hydraulic conductivity larger than $10^{-5}$ m/s. Additionally, a higher porosity and lower initial saturation of the adjacent rock mass promote both PWP dissipation and effective stresses development in backfill slurry, but their influences are relatively less pronounced compared to hydraulic conductivity of rock mass. Besides, the numerically simulated PWP and effective vertical stress were validated by comparisons with analytical results of Gibson model and modified Marston model, respectively. The findings are expected to provide valuable insights into the consolidation behaviour of tailings backfill slurry under field conditions and contribute reliable method for barricade design.*

**Keywords:** *tailings slurry, consolidation, porewater pressure, effective stress, rock mass drainage, FLAC3D*

## 1 Introduction

Mining methods with backfill have become one of the most widely adopted techniques in metal mines, as they not only address the challenges of tailings disposal on ground surface but also mitigate safety risks associated with excavated voids and increase ore recovery (Potvin et al. 2005; Guo et al. 2022; Ma et al. 2023).

The open stoping with subsequent backfill mining method effectively integrates the advantages of mining with backfill and open stoping, which represents the direction of green and mass mining in the future. In this method, the orebody can be divided vertically into a series of stages, separated by crown rock pillars to isolate mining activities. At each stage, the ore is further divided into primary and secondary stopes. The primary stope is first mined and filled with cemented backfill and must remain self-supporting during the recovery of secondary stopes. The cemented slurry undergoes settling, sedimentation, and consolidation processes to form artificial pillars (Liu et al. 2018; Ma et al. 2023). In contrast, secondary stopes are generally filled with uncemented backfill to reduce cement costs, as no further sidewall exposure is required.

[*] Corresponding author.

A critical challenge in secondary stope operations is ensuring barricade stability during and after the filling process, particularly while the uncemented backfill slurry is consolidating. The backfill slurry is mainly composed of tailings, which is the byproduct of mineral processing, mixed with water. While binders are added for cemented slurry in primary stopes, uncemented slurry for secondary stopes relies on the self-weight consolidation of the tailings-water mixture to gain strength. Backfill slurry is transported via pipelines to underground voids previously sealed by engineered structures known as barricades (Li & Yang 2015; Zheng & Li 2020). During and after filling, the barricade must remain stable until the backfill slurry achieves the desired consolidation state. To optimise the design of barricade loading capacity, it is essential to evaluate the evolution process of porewater pressure (PWP) within the uncemented slurry during and after filling, particularly in large-scale stopes such as longhole stage open stoping with subsequent backfill mining, where the magnitude of loading can be substantial (Grabinsky 2010).

The Gibson analytical model is commonly used to assess PWP during the consolidation of backfill slurry in mine stopes (Gibson 1958). Originally developed to investigate self-weight consolidation of accreting clay layers under one-dimensional assumptions, the Gibson model assumes impermeable side boundaries allowing water to drain only from the top and/or bottom planes. While more complex analytical models have been updated (Helinski et al. 2007, 2010; Fahey et al. 2010; Cui & Fall 2016; Zheng et al. 2018a, 2018b), such as those accounting for coupled thermal, hydraulic, mechanical, and chemical processes affecting slurry consolidation, they remain largely limited to describing one-dimensional consolidation behaviour and seldom consider influences of complex drainage boundaries encountered in practical stopes.

Numerical modelling has played as an effective tool for investigating the consolidation behaviour of backfill slurry in mine stopes. Previous studies have primarily focused on individual stopes, often simplifying the influences of adjacent rock mass as either fully impermeable or permeable drainage conditions along the side walls (El Mkadmi et al. 2013; Doherty 2015; Jaouhar et al. 2019). The consolidation process of backfill slurry in one stope surrounded by rock mass or cured backfill in adjacent stopes has not been adequately modelled or simulated.

In practice, backfill slurry in a stope is typically confined by the rock mass and/or cured backfill in neighbouring stopes. The rock mass often contains various geological faults, joints, and mining-induced cracks that act as seepage pathways for porewater from the backfill slurry. Clearly, the drainage properties of the adjacent rock mass, such as permeability, porosity, and initial saturation, can significantly affect the PWP dissipation and consolidation process of the slurry. Despite this, previous studies have typically modelled the surrounding boundaries as either fully impermeable or permeable boundaries for the backfill slurry. The impact of the rock mass' drainage properties on the stress state and consolidation behaviour of backfill slurry remains poorly understood and largely unclear.

In this study, numerical simulations were performed using FLAC3D to investigate the consolidation behaviours of uncemented backfill slurry in a vertical secondary stope confined by the rock mass with different drainage properties, including permeability, initial saturation, and porosity. The effects of these properties on PWP and effective stresses within the slurry were comprehensively analysed. The validation of the numerically simulated PWP and effective vertical stress were carried out by comparison with analytical results with Gibson model and modified Marston model, respectively.

# 2 Numerical model

## 2.1 Model construction and boundary conditions

Figure 1 illustrates the drainage and consolidation process of the uncemented slurry in a secondary stope surrounded by cured cemented backfill and/or fractured rock mass in open stoping with subsequent backfill mining. Porewater from the slurry can flow through fractures or voids in the adjacent rock mass or the cured backfill. Consequently, the drainage properties of the rock mass or cured backfill – especially cemented rockfill with various drainage paths, such as hydraulic conductivity, porosity ratio, and initial saturation – are expected to significantly influence the consolidation process of the backfill slurry.

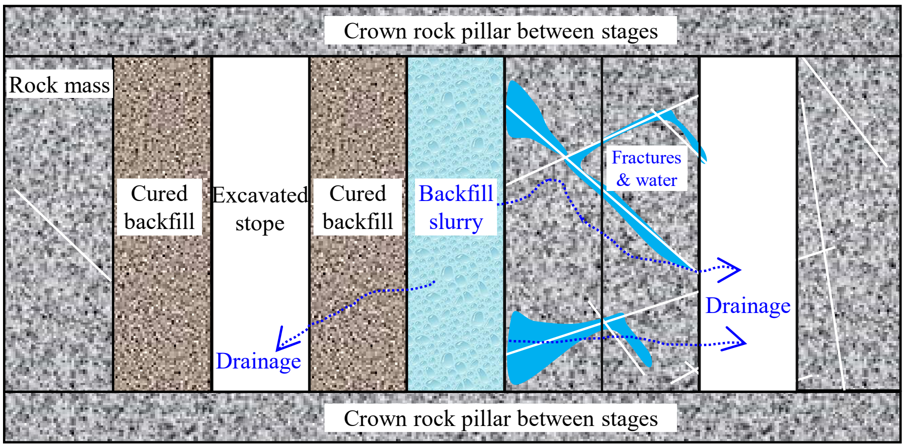


**Figure 1 Possible drainage paths for the porewater from the backfill slurry in one stope through adjacent rock mass and/or cured backfill in open stoping with subsequent backfill mining**

To investigate the impact of the drainage properties of the adjacent rock mass on the consolidation behaviour of the backfill slurry, a plane strain numerical model was constructed in FLAC3D, as shown in Figure 2. The model consists of an excavated stope with a width (*B*) and height (*H,)* surrounded by rock mass with a width (*W*). To improve computational efficiency, only half of the model is simulated, with a vertical symmetry plane (VSP) marked along the vertical central line of the stope width. The excavated stope is gradually filled with slurry, during which drainage and consolidation occur simultaneously. The stope filling process is modelled by continuously adding backfill layers at regular intervals until the slurry reaches the stope height. The rate of rise can be calculated as the height of each backfill layer divided by the time interval.

The bottom plane of the backfill slurry and rock mass (indicated by the red line) is modelled by fixed displacements in all directions and applied impervious hydraulic boundary. For the left-side plane of the filling slurry along the VSP (also marked by the red line), only the horizontal displacement in the normal direction is fixed, and the hydraulic boundary is set to be impermeable to simulate symmetry. For the right-side plane of the rock mass, indicated by the blue line, only the horizontal displacement is fixed, and the hydraulic boundary is set to be fully pervious to simulate free drainage conditions near the excavated stope voids. The top surface of the rock mass, marked by the red line, is free to move in all directions and has a waterproof boundary due to the presence of the crown rock pillar between 2 mining stages.

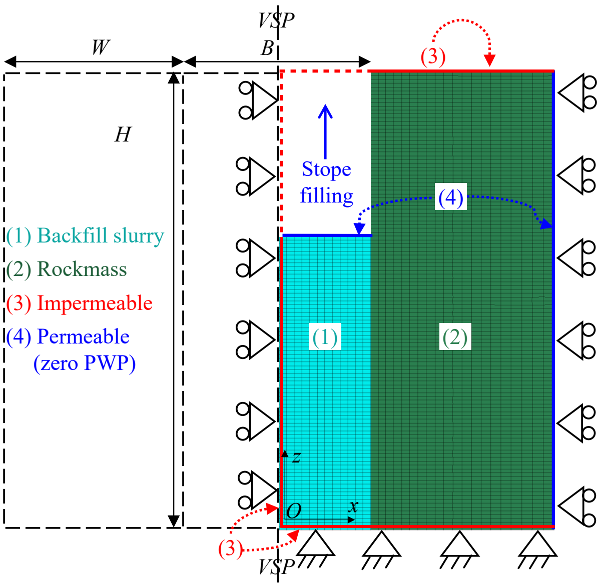


**Figure 2 Numerical model and boundary conditions constructed with FLAC3D**

A series of sensitivity analyses on model meshing in FLAC3D were performed to ensure stable numerical results and mesh independence. Hexahedral elements were selected due to their superior convergence performance and compatibility with the rectangular geometry of the model. The grid sizes were determined as 0.25 m in the *z*-direction and 0.5 m in the *x*-direction since the sensitivity tests indicated that further refinement below 0.25 m significantly increased computational costs without yielding perceptible changes in the results, suggesting that the chosen resolution is sufficient for numerical stability. A single-layer mesh with a thickness of 0.25 m was applied in the *y*-direction (perpendicular to the page), complemented by fixed y-displacement and impervious boundary conditions to simulate the plane strain condition in FLAC3D.

## 2.2 Material parameters and numerical cases

The backfill slurry and rock mass were assumed to be homogeneous, isotropic, and elasto-plastic materials governed by the Mohr–Coulomb failure criterion, with mechanical and hydraulic parameters summarised in Table 1. These typical values were primarily selected based on data reported in previous literature and partly derived from the authors' experiences gained during the implementation of several mining projects involving backfill (Ghirian & Fall 2013; Liu et al. 2016; Fan et al. 2025a, 2025b; Ma et al. 2026).

**Table 1 Mechanical and hydraulic parameters of the backfill slurry and rock mass**

| Items | Parameters | Symbols | Values | Unit |
|---|---|---|---|---|
| Uncemented backfill slurry | Dry density | $\rho_{df}$ | 1,500 | kg/m$^3$ |
| | Bulk modulus | $K_f$ | 480 | MPa |
| | Shear modulus | $G_f$ | 360 | MPa |
| | Cohesion | $c_f$ | 0 | MPa |
| | Internal friction angle | $\phi_f$ | 30 | ° |
| | Dilation angle | $\psi_f$ | 0 | ° |
| | Hydraulic conductivity | $k_f$ | $5\times10^{-6}$ | m/s |
| | Porosity ratio | $n_f$ | 50% | – |
| | Initial saturation ratio | $s_f$ | 100% | – |
| Rock mass | Dry density | $\rho_d$ | 2,700 | kg/m$^3$ |
| | Bulk modulus | $K$ | 2,800 | MPa |
| | Shear modulus | $G$ | 1,680 | MPa |
| | Cohesion | $c$ | 9.4 | MPa |
| | Internal friction angle | $\phi$ | 38 | ° |
| | Dilation angle | $\psi$ | 0 | ° |
| | Hydraulic conductivity | $k$ | *Variable* | m/s |
| | Porosity ratio | $n$ | *Variable* | – |
| | Initial saturation ratio | $s$ | *Variable* | – |
| Water | Density | $\rho_w$ | 1,000 | kg/m$^3$ |
| | Bulk modulus | $K_w$ | 2000 | MPa |
| Other | Gravitational acceleration | $g$ | 10 | m/s$^2$ |

Table 2 presents the simulation scenarios for the consolidation process of backfill slurry in mine stopes, considering the drainage properties of the adjacent rock mass. Case 0 is used to validate the numerical model by comparing the results with analytical solutions from Gibson and Marston models. Cases 1, 2, and 3 are designed to investigate the influence of the drainage properties of the adjacent rock mass on the consolidation behaviour of the backfill slurry by varying one parameter while keeping others constant.

**Table 2 Simulation scenarios for the consolidation process of backfill slurry in mine stopes considering the hydro-geotechnical properties of adjacent rock mass**

| Cases | Properties of rock mass laterally confining backfill slurry | | | | Hydraulic boundaries on side walls of filled stope |
|---|---|---|---|---|---|
| | Width, *W* (m) | Hydraulic conductivity, *k* (m/s) | Porosity ratio, *n* | Initial saturation ratio *s* | |
| 0 | 0 | – | – | – | Impermeable |
| 1 | 12 | $1\times10^{-5}$, $1\times10^{-6}$, $1\times10^{-8}$ | 25% | 40% | Based on assigned hydraulic properties of the rock mass. |
| 2 | 12 | $1\times10^{-6}$ | 10, 25, 40% | 40% | |
| 3 | 12 | $1\times10^{-6}$ | 25% | 40, 60, 100% | |

# 3 Numerical model verification

## 3.1 Comparisons between numerical results and Gibson model

The Gibson model is widely employed to analytically calculate the PWP of accreting sediment layers as they consolidate with increasing thickness (Gibson 1958). The model can serve as a benchmark to validate the reliability of numerical simulations on consolidation process of backfill slurry in a single stope during filling.

In the Gibson model, porewater is assumed to drain through the permeable top surface as the slurry height increases, while the side walls and base boundary are considered impermeable. The excess PWP, denoted as *u*, along the slurry height during consolidation can be determined using Equation 1:

$$u = \gamma' mt - \gamma'(\pi c_v t)^{-\frac{1}{2}} \left[\exp\left(\frac{-z^2}{4c_v t}\right)\right] \times \int_0^\infty \xi \tan h\left(\frac{m\xi}{2c_v}\right) \cos h\left(\frac{z\xi}{2c_v t}\right) \exp\left(-\frac{\xi^2}{4c_v t}\right) d\xi \tag{1}$$

where:

| | | |
|---|---|---|
| $u$ | = | excess PWP (kPa) |
| $h$ | = | current height of the slurry (m) |
| $z$ | = | elevation of the slurry (m) |
| $m$ | = | increasing rate of the slurry height (m/h) |
| $c_v$ | = | consolidation coefficient of the slurry (m²/h) |
| $\gamma'$ | = | effective unit weight of the filled slurry ($=\gamma_f - \gamma_w$, kN/m³) |
| $\gamma_f$ | = | unit weight of the filled slurry (kN/m³) |
| $\gamma_w$ | = | unit weight of the water (kN/m³) |
| $\xi$ | = | integral variable ($0 < \xi < \infty$). |

Furthermore, Gibson introduced a dimensionless time factor (*T*) to interpret the calculated results for the excess PWP at any given accreted thickness (*h*) and corresponding time (*t*) of the deposited slurry, as expressed in Equation 2.

$$T = \frac{m^2 t}{c_v} = \frac{m \times (m \times t)}{c_v} = \frac{m \times h}{c_v} \tag{2}$$

A numerical model was constructed in FLAC3D to simulate the consolidation behaviour of backfill slurry in one stope during filling. As shown in Case 0 of Table 1, the width of the surrounding rock mass (*W*) was set to zero, and impermeable boundaries were applied to the side walls and base plane. These configurations align with the assumptions of the Gibson model.

Figure 3 presents the comparison between the simulated excess PWP and the analytical solution under different time factors (*T*). As evident from Figure 3, there is strong agreement between the numerical and analytical results for the excess PWP across various stages of filling and consolidation, as represented by the time factor. These comparisons demonstrate that the numerical model developed in this study using FLAC3D is a reliable tool for investigating the excess PWP and consolidation process of backfill slurry in mine stopes during filling.

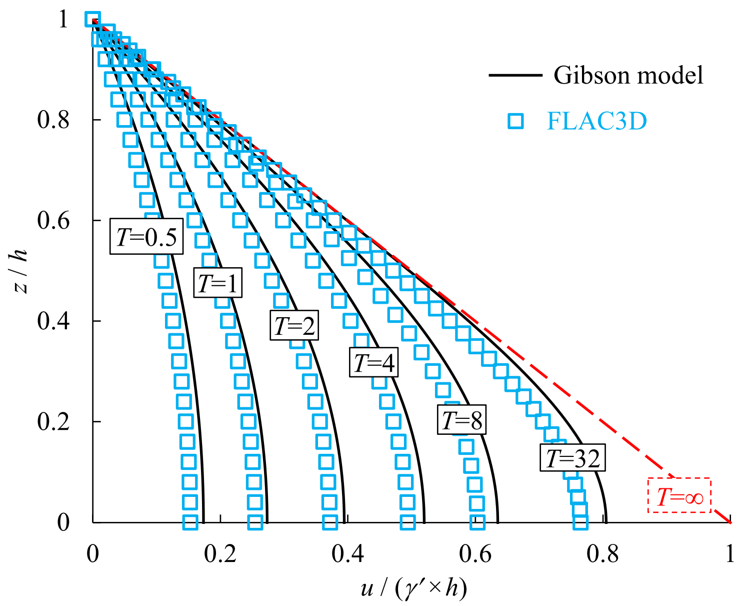


**Figure 3 Comparisons between simulated porewater pressure with analytical results with Gibson model at different time factor (*T*)**

## 3.2 Comparisons between simulated stresses and Marston model

The stress distribution within consolidating backfill slurry represents another key aspect that requires validation. For fully drained and consolidated dry granular materials, the Marston and Terzaghi models, originally derived from soil mechanics, have been widely used to calculate backfill stress distributions. Building on this foundation, Li & Aubertin (2009) further developed a modified analytical solution that accounts for the effects of PWP to evaluate the total and effective stresses in submerged cohesionless backfill. Equation 3 is suggested to analytically calculate the effective vertical stress $\sigma'_v$ (kPa) at a depth *h* (m) of the backfill in a mine stope with a width *B* (m), a totally filled stope height *H* (m) and a specified phreatic surface at vertical depth $H_p$ (m) from the top surface of backfill.

$$\sigma'_v = \frac{B\gamma_{subf}}{2K'_{sf}\tan\phi'_f}\left[1-\exp\left(-\frac{2K'_{sf}(h-H_p)}{B}\tan\phi'_f\right)\right] + \frac{\gamma_{mf}B}{2K_{sf}\tan\phi_f}\left[1-\exp\left(-\frac{2K_{sf}H_p}{B}\tan\phi_f\right)\right]\times\exp\left(-\frac{2K_{sf}(h-H_p)}{B}\tan\phi'_f\right) \tag{3}$$

where:

$\gamma_{subf}$ = unit weight of the submerged backfill under a phreatic surface ($=\gamma_{satf}-\gamma_w$, kN/m$^3$)

$\gamma_{satf}$ = unit weight of saturated backfill

$\gamma_w$ = unit weight of water

$\gamma_{mf}$ = unit weight of wet backfill above the phreatic surface (kN/m$^3$)

$K'_{sf}$ = effective coefficient of lateral earth pressure for the submerged backfill ($=\tan^2(45°-\phi'_f/2)$)

$K_{sf}$ = active coefficient of lateral earth pressure for the wet backfill ($=\tan^2(45°-\phi_f/2)$)

$\phi'_f$ = effective friction angle of the submerged backfill

$\phi_f$ = friction angle of wet backfill.

To validate the simulated effective stresses in FLAC3D, the vertical effective stresses along the VSP in the numerical model after the stope is fully filled (Case 0, Table 1) are compared with the analytical solutions derived from Marston model, as presented in Figure 4. It is evident that the simulated stresses at the moment the stope is just fully filled (0 days) are significantly lower than the analytical stresses, which assume a fully consolidated backfill. However, it is particularly noteworthy that as consolidation progresses over time, the simulated stresses along the stope height gradually increase and converge toward the analytical solution provided by Equation 3. These results clearly illustrate the gravity-driven consolidation process of the slurry, during which drainage dissipates excess PWP and increases effective stress. By 28 days after the stope is fully filled, the numerical and analytical stresses exhibit good agreement, particularly in the lower half of the stope, indicating that the backfill near the stope floor has reached a fully drained and consolidated state. However, the simulated stresses in the upper half of the stope at 28 days remain slightly lower than the analytical results, suggesting that additional time is required for the upper portion of the slurry to achieve full drainage and consolidation.

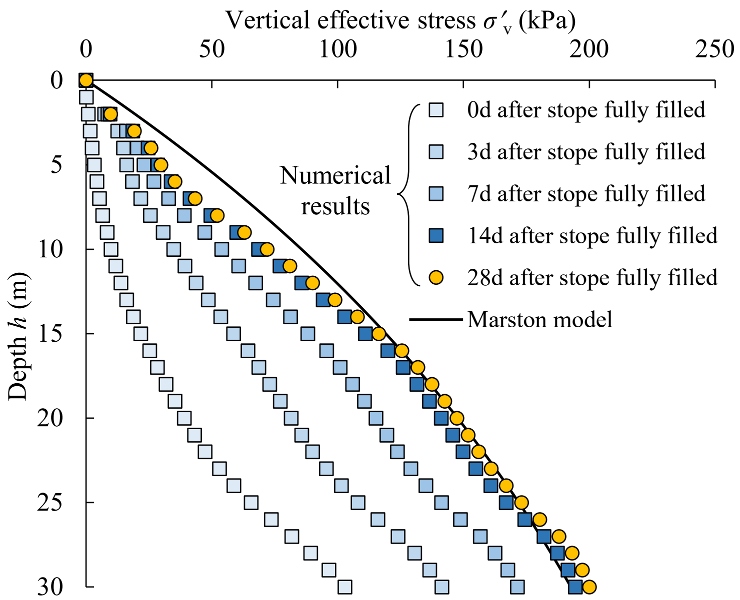


**Figure 4 Comparisons between effective vertical stresses obtained from Marston model and numerical results at different consolidating times after the stope was fully filled**

To further examine the temporal evolution of effective vertical stress and confirm its long-term stability, the numerical results monitored at the stope floor ($x$ = 0.75 m, $y$ = 1 m) are presented in Figure 5. It shows that effective vertical stress increases progressively from 0 to 28 days before reaching a distinct plateau, signifying a transition to a steady state. Beyond 28 days, the stress increment becomes negligible, rising only marginally from 205 to 206 kPa by 32.5 days. This trend confirms that stress has essentially stabilised after a 28-day consolidation period. Furthermore, when integrated with Figure 4, it can be concluded that the numerical results, once reaching this stable phase, demonstrate excellent agreement with the Marston model, thereby validating the accuracy of the simulation.

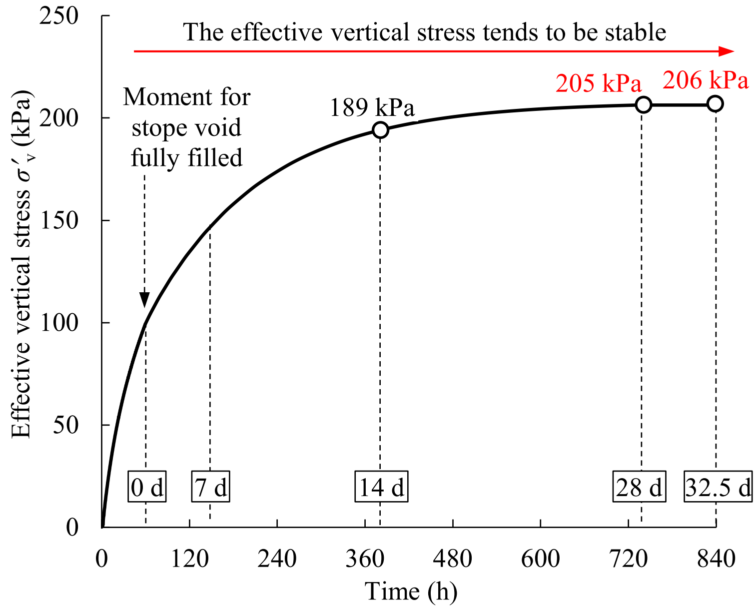


**Figure 5 Variations of effective vertical stress monitored at the bottom of the backfilled stope during and after the stope filling**

The comparisons presented in Figures 3 and 4 demonstrate that the numerical model developed using FLAC3D is capable of accurately simulating the PWP and effective stresses of backfill slurry in mine stopes across different stages of filling and consolidation. Subsequently, the numerical method is applied to investigate the consolidation process of uncemented backfill slurry in a mine stope considering the drainage properties of adjacent rock mass.

# 4 Effect of drainage properties of rock mass on backfill consolidation

## 4.1 Hydraulic conductivity

Figure 6 illustrates the evolution of PWP and vertical effective stresses monitored at the bottom of the backfilled stope surrounded by the rock mass with different hydraulic conductivity ($k$). For comparison, the results obtained from numerical models that do not consider the surrounding rock mass but instead assume an idealised impermeable or permeable boundary are also presented.

In Figure 6a, regardless of whether the backfilled stope is surrounded by rock mass or simplified as having an impermeable or permeable boundary, the PWP increases continuously during the filling process and reaches its peak value at the end of filling. Subsequently, the PWP gradually declines to a steady state over time. Notably, the PWP attains its minimum and maximum values during the filling process when the side walls are considered perfectly permeable and impermeable, respectively. The difference between their peak values can reach up to five-fold. This substantial discrepancy underscores that simplifying the adjacent rock mass as either perfectly permeable or impermeable in previous studies may introduce significant errors in estimating the PWP within the backfill slurry (El Mkadmi et al. 2013; Doherty 2015; Jaouhar & Li 2019).

When the influence of the adjacent rock mass on the drainage of the backfill slurry is taken into account, the PWP within the slurry decreases as the hydraulic conductivity of the rock mass increases. For rock masses with higher hydraulic conductivity, PWP dissipation occurs more rapidly following the end of filling. This indicates that higher permeability in the adjacent rock mass enhances drainage, thereby promoting the self-weight consolidation process of the slurry. It is also worth noting that the PWP evolution for the rock mass with a hydraulic conductivity of $10^{-5}$ m/s closely aligns with the results for the simplified permeable boundary, while the PWP behaviour for a hydraulic conductivity of $10^{-8}$ m/s is very similar to that of an impermeable boundary. This similarity suggests that, under specific conditions – namely, when the permeability of the adjacent rock mass is either very high or very low – the simplification of the rock mass as a permeable or impermeable boundary can serve as a reasonable approximation in numerical modelling. However, to achieve a more reliable and accurate estimation of PWP within the backfill slurry, precise modelling of the adjacent rock mass is required.

In Figure 6b, the vertical effective stresses increase steadily during the filling process before reaching a plateau. Additionally, with higher hydraulic conductivity of the adjacent rock mass, the vertical effective stresses exhibit a much steeper increase. Combined with the lower PWP for the higher hydraulic conductivity of the adjacent rock mass shown in Figure 6a, this suggests a load transfer from the porewater to the backfill matrix, resulting in the development of effective stresses. Since the rate of consolidation governs the rate of stress transfer to the backfill matrix, higher permeability of the surrounding rock mass facilitates the consolidation of the backfill slurry within one stope. Therefore, it is essential to consider the influence of the adjacent rock mass on the slurry consolidation behaviour, rather than simplistically treating it as a completely permeable or impermeable boundary, to achieve an accurate estimation of the stress state within backfill slurry.

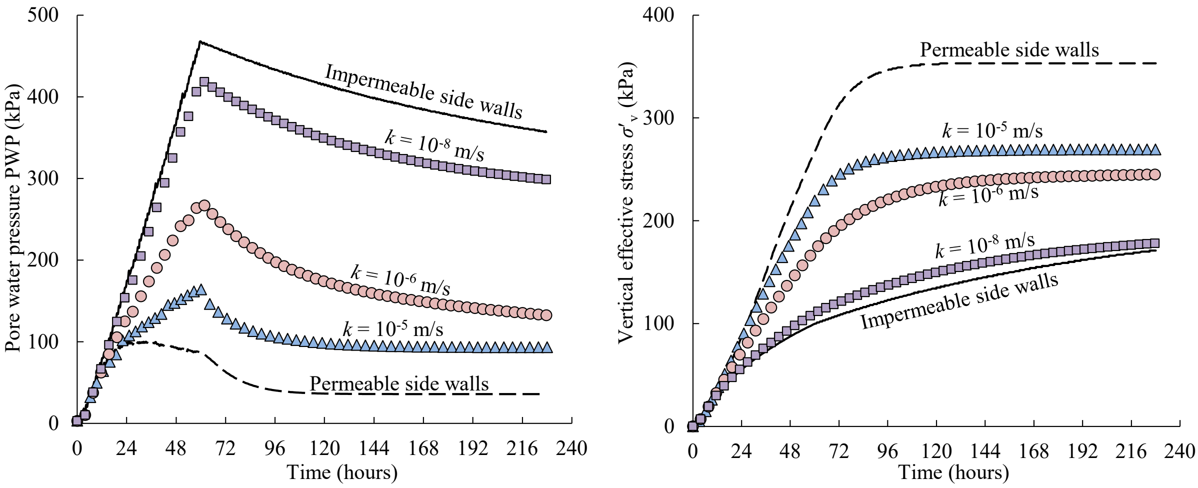


(a) (b)

**Figure 6 (a) Porewater pressure and (b) vertical effective stresses within the backfill slurry monitored near the bottom of the stope confined by the rock mass with varied hydraulic conductivity**

## 4.2 Porosity ratio

Figure 5 shows the evolution of PWP and vertical effective stresses monitored at the bottom of the backfilled stope surrounded by the rock mass with porosity of 10, 25, and 40%. The results obtained from numerical models with the permeable and impermeable side walls are also included for comparison.

As shown in Figure 7a, the PWP increases markedly throughout the stope filling stage, reaching its peak at the end of filling, after which it steadily declines. In contrast, Figure 7b shows that the vertical effective stresses increase steadily and smoothly once the backfill is placed within the stopes. These trends illustrate the load transfer from the porewater to the backfill matrix during the consolidation of backfill slurry. Clearly, a higher porosity of the adjacent rock mass facilitates both PWP dissipation and the development of effective stresses. This phenomenon occurs because a higher porosity in adjacent rock mass provides additional void space to accommodate porewater draining from the backfill slurry, thereby enhancing promoting the consolidation process.

In practice, the porosity of rock mass can vary widely, from nearly 0 to over 90% (Goodman 1991), depending on factors such as mineral composition, depth, and geological structures (e.g. joints and fractures). The voids present in the adjacent rock mass serve as storage spaces and seepage pathways for porewater expelled from the backfill slurry during consolidation. As observed in Figure 7, a significant discrepancy exists between the results for the backfill slurry confined by rock mass with varying porosities and those for cases involving impermeable or permeable side walls. This highlights the substantial influence of the porosity of adjacent rock mass on the consolidation behaviour. An impermeable boundary assumes negligible water storage capacity in the adjacent rock mass, while a permeable boundary implies unlimited water storage capacity. However, neither scenario accurately reflects actual conditions.

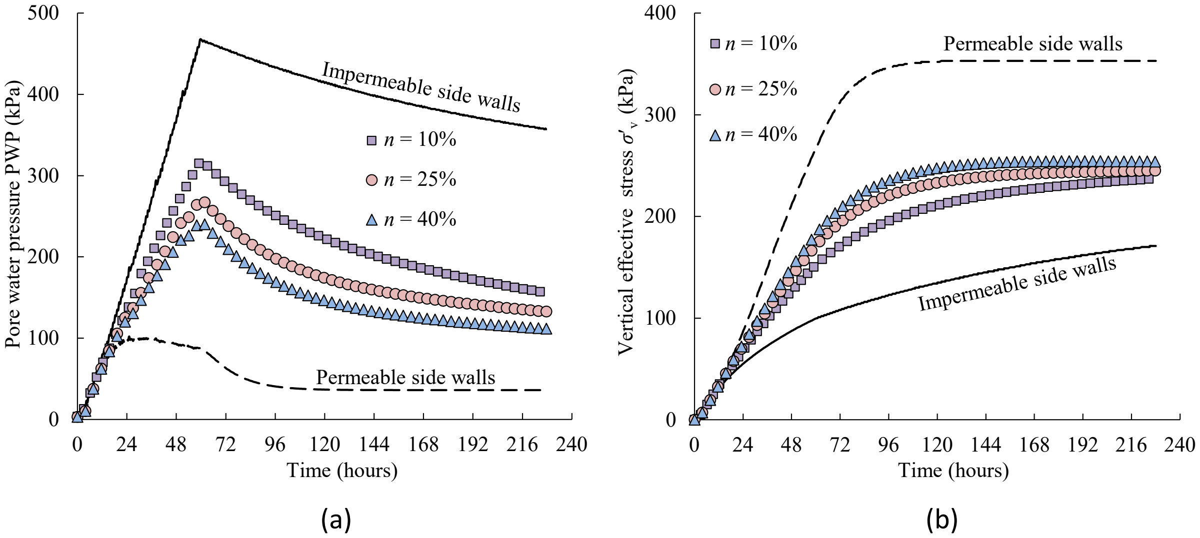


**Figure 7 (a) Porewater pressure (PWP) and (b) vertical effective stresses within the backfill slurry monitored near the bottom of the stope confined by the rock mass with varied porosity ratio**

## 4.3 Initial saturation

Figure 6 shows the evolution process of PWP and vertical effective stresses monitored at the bottom of the backfilled stope surrounded by the rock mass with initial saturation of 40, 60, and 100%. For comparison, results obtained from numerical models with permeable and impermeable side walls are also presented.

As shown in Figure 8a, the PWP increases with the initial saturation of the rock mass, while the vertical effective stresses in Figure 8b exhibit an opposite trend. This behaviour can be attributed to the fact that initial saturation reflects the initial water storage capacity of the rock mass at a given porosity. When the backfill slurry is confined by rock mass with the high initial saturation (e.g. $s$ = 100%), porewater drained from the slurry cannot easily flow into the adjacent rock mass, as the drainage of pre-existing water within the surrounding rock also requires time. Conversely, rock mass with the low initial saturation has greater available storage capacity, allowing porewater from the backfill slurry to drain more readily into it. This promotes drainage, accelerates PWP dissipation, and facilitates the development of effective stresses during consolidation as the initial saturation of the rock mass decreases.

In Figure 8, a notable discrepancy is observed between the PWP and effective stresses within the backfill slurry surrounded by the rock mass with different initial saturation and the corresponding values under impermeable and permeable side walls. These pronounced differences highlight the necessity of considering the saturation of the adjacent rock mass when estimating the PWP or effective stress of the backfill slurry for barricades design. This consideration is particularly critical in extreme mining environments, such as arid desert regions where the rock mass is typically less saturated, or groundwater-rich areas where the rock mass may be fully saturated.

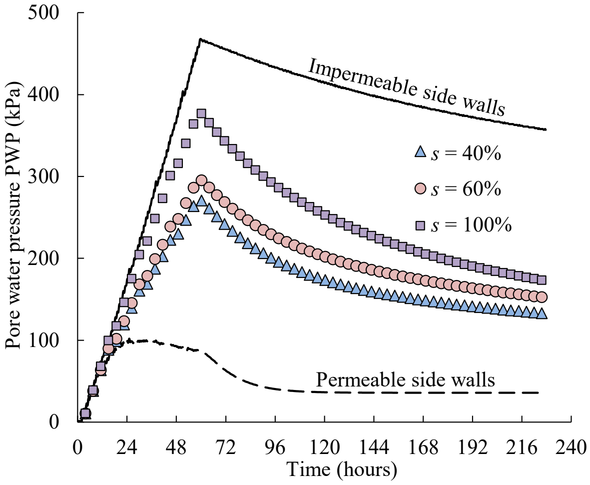


(a)

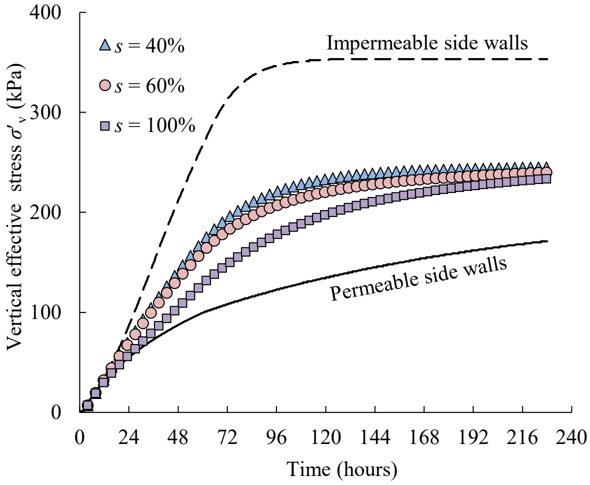


(b)

**Figure 8 (a) Porewater pressure (PWP) and (b) vertical effective stresses within the backfill slurry monitored near the bottom of the stope confined by the rock mass with varied initial saturation**

# 5 Conclusion

Numerical simulations were conducted with FLAC3D to investigate evolution process of PWP and effective stress of uncemented backfill slurry in a vertical stope considering adjacent rock mass with different hydraulic conductivity, initial saturation, and porosity. The main conclusions are summarised as follows:

1. When the adjacent rock mass is considered, the PWP within backfill slurry are consistently higher than those from models assuming fully permeable boundaries but lower than those assuming impermeable boundaries. Neglecting the adjacent rock mass leads to either overly conservative or excessively aggressive stress estimates. Accurate stress prediction requires proper consideration of the adjacent rock mass.
2. A high hydraulic conductivity in the adjacent rock mass accelerates backfill slurry consolidation. At low conductivity ($10^{-8}$ m/s), PWP and effective stress evolution match impermeable boundary behaviour; at high conductivity ($10^{-5}$ m/s), they approach permeable boundary conditions. In these extremes, the surrounding rock mass can reasonably be simplified as a hydraulic boundary.
3. Higher porosity and lower initial saturation of the adjacent rock mass both promote the PWP dissipation and effective stresses development in backfill slurry. In arid desert or groundwater-rich regions, the adjacent rock mass may lead considerable impacts to the consolidation of the backfill slurry.
4. The findings suggest that considering the influence of the hydro-geotechnical properties of adjacent rock mass on the backfill consolidation allows for a more accurate evaluation of PWP and total stresses, which is critical for a more cost-effective barricade design. Furthermore, the validated numerical method provides a reliable tool for practical mine design, which can offer guidance on operational parameters such as the rate of rise and individual pour heights to ensure the safety of filling operations.

# Acknowledgement

This research was funded by the Deep Earth Probe and Mineral Resources Exploration — National Science and Technology Major Project (Grant No. 2024ZD1003705) and the Beijing Nova Program (Grant No. 20220484057).

# References

Cui, L & Fall, M 2016, 'Multiphysics model for consolidation behavior of cemented paste backfill', *International Journal of Geomechanics*, vol. 17, no. 3, pp. 1–23.

Doherty, J 2015, 'A numerical study into factors affecting stress and pore pressure in free draining mine stopes', *Computers and Geotechnics*, vol. 63, no. 1, pp. 331–341.

El Mkadmi, N, Aubertin, M & Li, L 2013, 'Effect of drainage and sequential filling on the behavior of backfill in mine stopes', *Canadian Geotechnical Journal*, vol. 51, no. 1, pp. 1–15.

Fahey, M, Helinski, M & Fourie, A 2010, 'Consolidation in accreting sediments: Gibson's solution applied to backfilling of mine stopes', *Geotechnique*, vol. 60, no. 11, pp. 877–882.

Fan, C, Li, L, Yang, XC, Liu, GS, Guo, LJ & Tang, J 2025a, 'Analytical solution for determining wall closure associated with stope excavation underneath sill mat constructed by cemented backfill', *Journal of Rock Mechanics and Geotechnical Engineering*, vol. 17, no. 2, pp. 983–995.

Fan, C, Li, L, Yang, XC, Liu, GS, Guo, LJ & Tang, J 2025b, 'Analytical solution for estimating the minimum required strength of sill mat by considering failure due to rock wall closure', *Journal of Rock Mechanics and Geotechnical Engineering*, vol. 17, no. 2, pp. 996–1007.

Ghirian, A & Fall, M 2013 'Coupled thermo-hydro-mechanical–chemical behaviour of cemented paste backfill in column experiments. Part I: physical, hydraulic and thermal processes and characteristics', *Engineering Geology*, vol. 164, no. 17, pp. 195-207.

Gibson, RE 1958 'The progress of consolidation in a clay layer increasing in thickness with time', *Geotechnique*, vol. 8, no. 4, pp. 171–182.

Goodman, RE 1991, *Introduction to Rock Mechanics*, John Wiley & Sons, Hoboken.

Grabinsky, MW 2010, 'In situ monitoring for ground truthing paste backfill designs', in R Jewell & AB Fourie (eds), *Paste 2010: Proceedings of the Thirteenth International Seminar on Paste and Thickened Tailings*, Australian Centre for Geomechanics, Perth, pp. 85–98, https://doi.org/10.36487/ACG_rep/1063_8_Grabinsky

Guo, LJ, Liu, GS, Ma, QH & Chen, XZ 2022, 'Research progress on mining with backfill technology of underground metalliferous mine', *Journal of China Coal Society*, vol. 47, no. 12, pp. 4182–4200.

Helinski, M, Fahey, M & Fourie, A 2007, 'Numerical modeling of cemented mine backfill deposition'. *Journal of Geotechnical and Geoenvironmental Engineering*, vol. 133, no. 10, pp. 1308–1319.

Helinski, M, Fahey, M & Fourie, A 2010, 'Coupled two-dimensional finite element modelling of mine backfilling with cemented tailings', *Canadian Geotechnical Journal*, vol. 47, no. 11, pp. 1187–1200.

Jaouhar, EM & Li, L 2019, 'Effect of drainage and consolidation on the porewater pressures and total stresses within backfilled stopes and on barricades', *Advances in Civil Engineering*, p. 1802130.

Li, L & Yang, PY 2015, 'A numerical evaluation of continuous backfilling in cemented paste backfilled stope through an application of wick drains', *International Journal of Mining Science and Technology*, vol. 25, no. 6, pp. 897–904.

Li, L & Aubertin, M 2009, 'Influence of water pressure on the stress state in stopes with cohesionless backfill', *Geotechnical and Geological Engineering*, vol. 27, no. 1, pp. 1–11.

Liu, GS, Li, L, Yang, CX & Guo, LJ 2018, 'Required strength estimation of a cemented backfill with the front wall exposed and back wall pressured', *International Journal of Mining and Mineral Engineering*, vol. 9, no. 1, pp. 1–20.

Liu, GS, Li, L, Yang, CX & Guo, LJ 2016, 'Stability analyses of vertically exposed cemented backfill: A revisit to Mitchell's physical model tests', *International Journal of Mining Science and Technology*, vol. 26, no. 6, pp. 1135–1144.

Ma, QH, Liu, GS, Yang, XC & Guo, LJ 2023. 'Physical model investigation on effects of drainage condition and cement addition on consolidation behavior of tailings slurry within backfilled stopes', *International Journal of Minerals, Metallurgy and Materials*, vol. 30, no. 8, pp. 1490–1501.

Ma, QH, Liu, GS, Yang, XC, Guo, LJ & Fourie, A 2026, 'Stability of base-exposed backfill roof considering interfaces between adjacent drifts in underhand drift-and-fill mining', *Journal of Rock Mechanics and Geotechnical Engineering*, vol. 2026, no. 18, pp. 214–229.

Potvin, YH, Thomas, E & Fourie, A 2005, *Handbook on Mine Fill*, Australian Centre for Geomechanics, Perth.

Zheng, J & Li, L 2020, 'Experimental study of the "short-term" pressures of uncemented paste backfill with different solid contents for barricade design', *Journal of Cleaner Production*, vol.275, no. 1, p. 123068.

Zheng, J, Li, L, Mbonimpa, M & Pabst, T 2018a, 'An analytical solution of Gibson's model for estimating the pore water pressures in accreting deposition of slurried material under one-dimensional self-weight consolidation. Part II: impervious base', *Indian Geotechnical Journal*, vol. 48, no. 1, pp. 72–83.

Zheng, J, Li, L, Mbonimpa, M & Pabst, T 2018b, 'An analytical solution of Gibson's model for estimating the pore water pressures in accreting deposition of slurried material under one-dimensional self-weight consolidation. Part II: impervious base', *Indian Geotechnical Journal*, vol. 48, no. 1, pp. 188–195.